

## Conformationally constrained analogues of endogenous tripeptide inhibitors of zinc metalloproteinases

Silvana D'Alessio<sup>a</sup>, Carlo Gallina<sup>b\*</sup>, Enrico Gavuzzo<sup>c</sup>, Cesare Giordano<sup>d</sup>, Barbara Gorini<sup>e</sup>,  
Fernando Mazza<sup>e</sup>, Mario Paglialonga Paradisi<sup>d</sup>, Gabriella Panini<sup>d</sup>, Giorgio Pochetti<sup>c</sup>

<sup>a</sup>Polifarma Research Center, Via Tor Sapienza 138, 00185 Rome, Italy

<sup>b</sup>Dipartimento di Scienze del Farmaco, Istituto di Scienze del Farmaco, Università G. d'Annunzio,  
Via dei Vestini, 66100 Chieti, Italy

<sup>c</sup>Istituto di Strutturistica Chimica del CNR, C.P. n. 10, 00016 Monterotondo Stazione, Rome, Italy

<sup>d</sup>Centro di Studio per la Chimica del Farmaco del CNR, Università La Sapienza, P. le A. Moro 5, 00185 Rome, Italy

<sup>e</sup>Dipartimento di Chimica, Ingegneria Chimica e Materiali, Università degli Studi, 67010 L'Aquila, Italy

Received 10 September 1999; accepted 11 September 2000

**Abstract** – Two diastereomeric furan-2-carboxylamino-3-oxohexahydroindolizino[8,7-*b*]indole carboxylates, highly constrained analogues of endogenous pyroglutamyl tripeptide inhibitors of snake venom endopeptidases, have been prepared as potential inhibitors of adamalysin II and matrix metalloproteinases. They proved to be inactive against adamalysin II and weak inhibitors of gelatinase A, gelatinase B, stromelysin 1 and human neutrophil collagenase. Evaluation of the mode of binding of the (2*R*,5*S*,11*bR*) isomer in the active site of adamalysin II suggests that the decrease of potency may be due to the reorientation of the acylamino chain in three of the heterocyclic nucleus, to a short contact at the entrance of the S<sub>1</sub>' hydrophobic cleft and to the loss of flexibility of the tetracyclic nucleus in the P<sub>1</sub>, P<sub>2</sub> region of the inhibitor, which prevents optimal arrangement in the S<sub>1</sub>' specificity subsite. © 2001 Éditions scientifiques et médicales Elsevier SAS

2-acylamino-3-oxohexahydroindolizino[8,7-*b*]indole carboxylates / crystal structure / adamalysin II / matrix metalloproteinases

### 1. Introduction

The matrix metalloproteinases (MMPs) are a family of zinc endopeptidases [1] involved in tissue remodelling and connective tissue turnover. Aberrant regulation of these enzymes, particularly collagenases, stromelysins and gelatinases, has been implicated in several pathologies [2–5] including rheumatoid arthritis and tumour invasion and metastasis. Thus, inhibition of MMPs enzymatic activity has become an important pharmacological target for the treatment of a range of diseases for which no specific or effective drugs are available.

Many structural classes of potent MMP inhibitors [2–10] incorporate a substrate-like peptide chain,

which binds in the enzyme active site and a zinc binding function, mainly hydroxamate, carboxylate, phosphonate and phosphinate, which interacts with the catalytic zinc ion. Peptide derived inhibitors, however, generally suffer from undesirable physical properties, mainly poor solubility, low stability to hydrolytic enzymes, fast biliary clearance and poor oral availability. Therefore, design and synthesis of non-peptidic MMP inhibitors, suitable as drug candidates, has grown as an active research field. Herein, we report on structural modifications of endogenous snake venom peptides, pointing to generate non-peptidic, conformationally constrained inhibitors of matrix and snake venom metalloproteinases.

On the basis of common structural and functional properties, snake venom hemorrhagic zinc endopeptidases, named reprotins, have been grouped in the superfamily of metzincins [11], together with astacins,

\* Correspondence and reprints.

E-mail address: cgallina@unich.it (C. Gallina).

serralysins and MMPs. The crystal structure [12, 13] of adamalysin II, a reprotolysin from *Crotalus adamanteus*, shows highly conserved overall topology with MMPs, namely MMP-8 and very close similarity at the active site. The catalytic domains of all these enzymes contain an essential zinc ion coordinated by the imidazole groups of three conserved histidine residues of the consensus sequence HEXXHGXHH, lying at the bottom of the binding cleft. They present substantially identical core structures, while important variations in the surface loops originate considerable differences in the specificity subsites. The S<sub>1</sub>' subsite, generally consisting of hydrophobic residues, varies considerably in size and shape and is considered to be the primary specificity site, since it can strongly influence recognition of substrates and inhibitors.

Small pyroglutamyl peptides are present in millimolar concentration, together with reprotolysins, in the crude venom of crotalides [14]. Two of these endogenous peptides, pyroGlu–Asn–Trp–OH and pyroGlu–Glu–Trp–OH, isolated from the venom of *C. atrox*, were demonstrated to be inhibitors of atrolysin

in the low micromolar range [15] and it has been proposed that they may function as temporary inhibitors of the venom proteinases during storage in the snake glands. Structural basis for binding interactions of pyroglutamyl tripeptides with metalloproteinases has been clarified by solution of the crystal structure of the pyroGlu–Asn–Trp–OH atrolysin C complex [16].

Owing to the close resemblance between reprotolysins and MMPs, snake venom pyroglutamyl peptides and their analogues have been previously studied as inhibitors of the human zinc proteinases [15]. The phosphonate ligand **1a**, as well as the carboxylate analogues **1b** and **2** (figure 1), are examples of metalloproteinase inhibitors obtained by structural variation of pyroGlu–Asn–Trp–OH. Crystal structures of adamalysin II complexed with phosphonate **1a** [17] and with carboxylates **1b** and **2** [18] have been used as starting models for the conformationally constrained, non-peptidic analogous **4a**, as a possible inhibitor of adamalysin II and MMPs.

Cyclization of the Trp based carboxylate inhibitor **1b** into the cyclo-Trp analogue **2**, by means of a

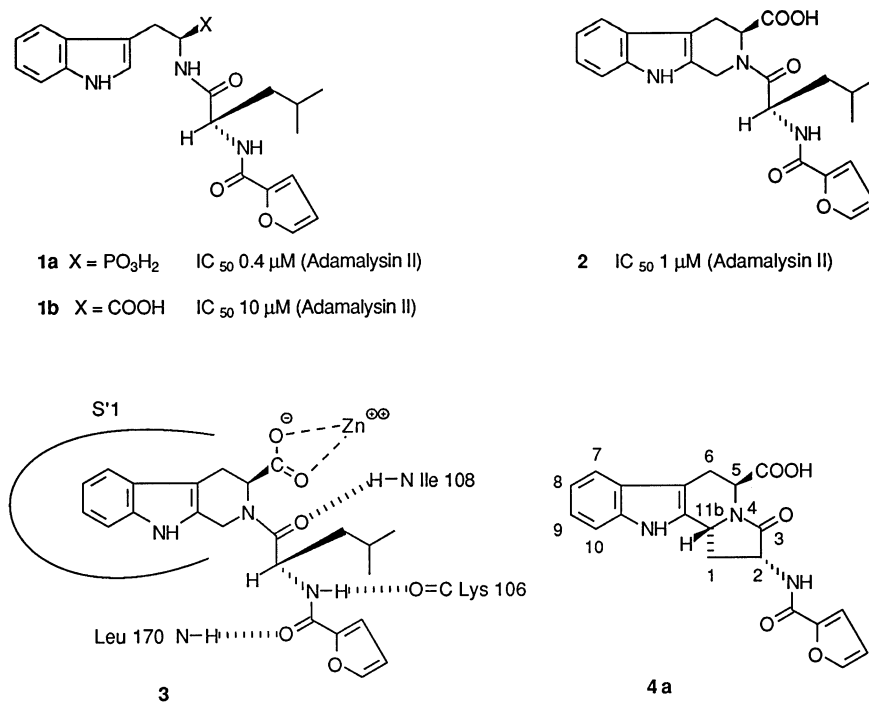


**Figure 1.** Linear (**1a**, **1b**), tricyclic (**2**) and tetracyclic (**4a**) inhibitors of zinc-proteinases. Key bonding interactions in the complex of **2** with adamalysin II, involving the large hydrophobic pocket in S<sub>1</sub>', the catalytic zinc ion and the residues Lys-106, Ile-108 and Leu-170 of the enzyme, are reported in the schematic representation **3**.

methylene group joining the tryptophan amino group with the indole 2 position, caused an increase of the binding affinity for adamalysin II of one order of magnitude [18]. Since both **1b** and **2** inhibitors bind in the active site of the enzymes, adopting substantially identical conformations [18], the increase of potency of the cyclic analogue can be attributed to the decrease of conformational entropy for the protease binding. The schematic representation **3** illustrates the key enzyme–inhibitor interactions observed in both the crystal structures [18]. The carboxylate oxygens legate the catalytic zinc ion in a bidentate mode, while the Trp side chain partly fills the primary specificity subsite  $S_1'$ . Leu CO, Leu NH and furan-2-carbonyl CO groups form H-bonds with complementary functions of the protein. The Leu side chain and the furan ring are involved in loose binding interactions with the surrounding groups.

The distance between Leu  $\alpha$ CH and the bridge methylene carbon in the binding conformation **3** is ca. 2.9 Å. Joining of these carbons with a new methylene bridge shortens the distance to 2.4 Å. This cyclization, combined with deletion of the Leu side chain, leads to the conformationally constrained analogue **4a**, where the cyclo-Trp unit of **2** is replaced with the highly constrained 2-amino-3-oxohexahydroindolizino[8,7-*b*]indole-5-carboxylate skeleton. In a putative complex of **4a** in the adamalysin II active site, all the binding interactions represented in **3** could be only slightly modified, provided that the 2, 5 and 11*b* stereogenic centres are in the *S*, *R*, *S* configuration.

This additional cyclization points to the preorganization of the ligand into a conformation allowing zinc coordination by the carboxylate and burying of the heterocyclic moiety into the hydrophobic cleft in  $S_1'$ . Since this subsite involves a large area of interaction, presenting different residues and different capacity of reorganization upon ligand binding in the various MMPs, it was expected that the increase of rigidity of the molecule could greatly affect the potency and selectivity of the inhibitor. It could be anticipated, however, that the increase in size due to the 1-methylene group would require a small opening of the protein chain at the entrance of the hydrophobic cleft in order to allow the accommodation of the more bulky heterocyclic nucleus. Additional changes concern the conformational preferences of the furan-2-carbonylamino chain that would be affected by the creation of the new ring. In order to evaluate the effects on binding of this conformational restriction,

we decided to embark on the preparation of the (2*R*,5*S*,11*bR*)-2-(furan-2-carbonyl)amino-5-carboxy-3-oxo-2,3,5,6,11,11*b*-hexahydro-1*H*-indolizino[8,7-*b*]indole **4a**. This highly constrained heterocyclic nucleus could supply a new scaffold for non-peptide inhibitors of adamalysin II and MMPs. The (2*S*,5*S*,11*bR*) stereo isomer **4b** (figure 2) was also prepared to evaluate the consequence of the change of configuration at the **2** position.

## 2. Chemistry

The two desired compounds **4a** and **4b** were prepared by following previously reported [19] procedures for synthesis of 2-benzyloxycarbonylamino-3-oxo-11*b*-hexahydroindolizino[8,7-*b*]indole-5-carboxylate nucleus with complete control of the stereochemistry (figure 2).

Reaction of *N*-benzyloxycarbonyl-D-homoserine aldehyde benzyloxy ester **5a** with H-L-Trp-OMe, under conditions of kinetic control [20, 21] of the Pictet–Spengler reaction, gave a mixture of the *trans* (**6a**) and *cis* (**6c**)  $\beta$ -tetrahydrocarbolines, richer in the *cis*, less stable isomer. The *trans* lactame **7a**, required for our purposes, derives from the less abundant, more stable carboline **6a**, which could not be separated from the prevailing diastereoisomer **6c**, by standard chromatographic procedures. Therefore, the **6ac** mixture was directly refluxed in toluene in the presence of 10 molar equiv. of trifluoroacetic acid. Under conditions of acid catalysis, the **6ac** kinetic mixture richer in the *cis* carboline **6c** was transformed into a **7ac** mixture richer in the more stable *trans* lactame **7a**, which could be secured by silica-gel chromatography. Tetrahydro  $\beta$ -carboline **6b** and lactame **7b** were prepared as previously reported [19].

Conversion of esters **7a** and **7b** into the carboxylic acids **4a** and **4b** required three steps: (1) hydrogenolysis of the benzyloxycarbonyl group by using ammonium formate in the presence of *Pd/C*; (2) acylation of the resulting amines with furan-2-carboxylic acid by dicyclohexylcarbodiimide/1-hydroxybenzotriazole activation [22]; and (3) hydrolysis of the methylesters **8a** and **8b** under mild alkaline conditions [19]. Stereochemistry of intermediate and final compounds has been attributed on the basis of  $^1\text{H}$  NMR spectra, taking into account the assignments for the previously reported carbolines **6b**, **6d** and lactames **7b** and **7d** [19].

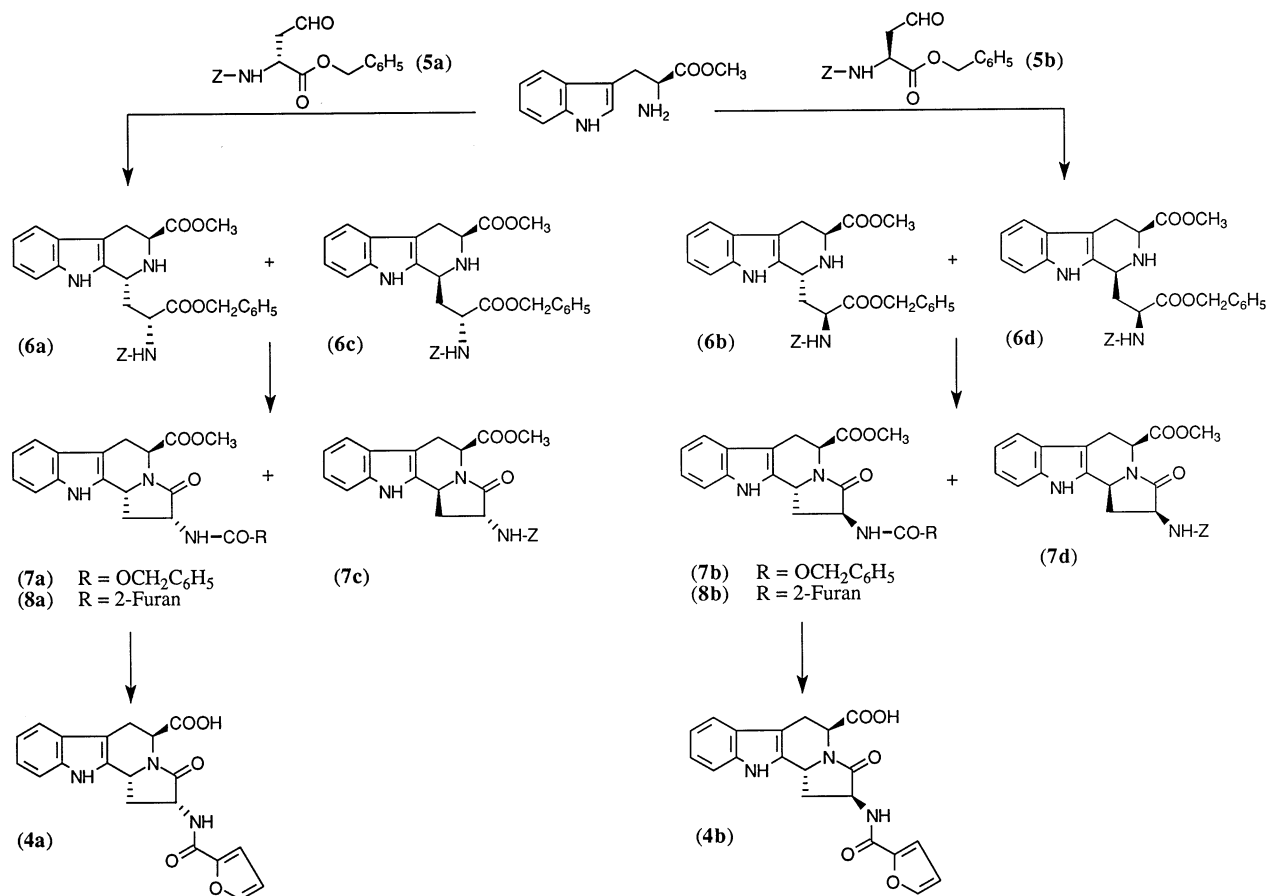


**Figure 2.** Synthesis of the diastereomeric furan-2-carbonylamino-3-oxohexahydroindolizino[8,7-*b*]indole carboxylates **4a** and **4b**.

### 3. X-ray analysis

With the aim to unequivocally confirm the configuration at the 2, 5 and 11*b* stereogenic centres of the tetracyclic compound **4a**, and also to determine its solid-state conformation for comparison with the binding conformation of **2** in the active site of adamalysin II, the present X-ray analysis was performed on crystals of **4a**.

A perspective view of the molecular conformation of **4a**, together with adopted numbering scheme (top) and the relevant internal torsion angles of C and D rings (bottom) are reported in *figure 3*. The pentatomic D ring is characterized by a pseudomirror plane bisecting the amide bond and passing through the C2 atom; its conformation can be described by an envelope with the C1 atom at the flap, displaced of 0.369 Å from the plane of the other four ring atoms, on the opposite side of the H bound to the C11*b*. The hexatomic C ring

presents a pseudomirror plane passing through the C5 and C16 atoms; its conformation can be described as a sofa with the C5 atom displaced of 0.606 Å from the plane of the other five ring atoms, on the same side of the H bound to C11*b*. The fusion between C and D rings is of the *quasi-trans* type, since the internal torsion angles of junction have opposite signs, being  $-18.8$  and  $34.0^\circ$  for the penta and hexa-atomic rings, respectively. The carboxyl group is axial and lies on the same side of the H bound to C11*b*. The equatorial character of the furan-2'-carbonylamino moiety is weakened by the low puckering of the pentatomic ring; the two torsion angles preceding and following the carbon bound to the furan ring are  $11.8$  and  $-21.1^\circ$ , respectively. The endocyclic amide bond is slightly distorted from *trans* planarity, the torsion angle C2–C3–N4–C5 being  $-169.7^\circ$ ; this small torsion, however, is not caused by non-planarity of nitrogen, since the sum of valence angles around its three substituents is  $359.6^\circ$ .



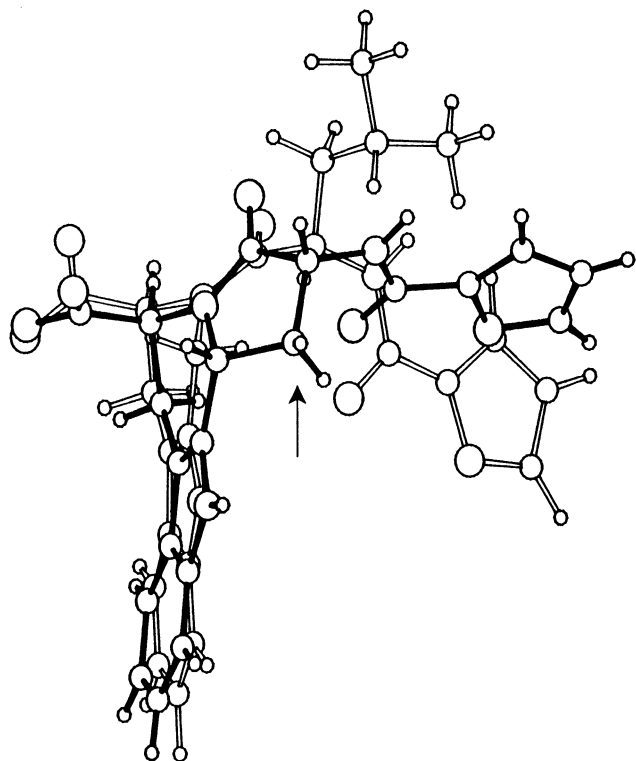


**Figure 4.** Best fitting between small-molecule crystal structure of **4a** (filled bonds) and crystal structure of **2** in the complex with adamalysin II, based on the carboxylate carbon and C5, C7 and C10 atoms. An arrow indicates the  $\beta$ -hydrogen at C1 forming a short contact (ca. 2 Å) with the carbonyl oxygen of Pro-168 in the putative complex with the enzyme.

nuclei and carboxylate groups are practically overlapping. Both the C2 carbon and the adjacent NH of **4a**, are very close to the positions of the corresponding atoms of **2**, confirming the desired preorganization of the constrained ligand according to the binding conformation of **2**. These features would guarantee contemporary occupation of the  $S'_1$  specificity site, zinc chelation and orientation of the acylamino chain toward the  $S'_2, S'_3$  sites. However, the C1 methylene bridge, indicated with an arrow, increases size and rigidity of the molecule in the  $P'_1, P'_2$  region and determines a preferred conformation of the furan-2-carbonylamino chain ca.  $90^\circ$  rotated around the C2–N19 bond.

It has been recently pointed out that metalloproteinases, as well as aspartic, serine and cysteine proteinases, require an extended  $\beta$ -strand conformation for their active site directed inhibitors and substrate analogues [23]. Accordingly, the crystal

structures of the known inhibitors **1a**, **1b** and **2** in the adamalysin II active site show that the acylamino chains, involved in H-bonds with Leu-170 NH and Lys-106 CO of the protein, adopt extended  $\beta$ -strand conformations. In a putative complex containing the crystal conformation of **4a** in the active site of adamalysin II, these H-bonds would be lost and could only be restored at the energetic cost required by the reorientation of the chain [24].

The putative complex of the crystal conformation of **4a** in the active site of adamalysin II also shows that the  $\beta$  hydrogen at C1 is too close (ca. 2 Å distance) to the carbonyl oxygen of Pro-168, giving rise to an unfavourable nonbonded contact. It has been reported [25] that the carbonyl oxygen of Pro-238 in MMP-1, homologous of Pro-168 in adamalysin II, can undergo a small but significant displacement in order to avoid unacceptable contacts with groups of the inhibitor, providing evidence for flexibility of the protein chain in this region. Analogous flexibility of the protein in MMP-3, MMP-8 and MMP-9 could possibly explain the residual inhibiting activity shown by **4a** against these enzymes. The loss of measurable affinity for adamalysin II could be attributed to larger rigidity of the homologous chain in this enzyme.

Not only the protein chain, but also the inhibitor flexibility, can strongly affect enzyme affinity. Previous work, both in the field of metalloproteinases [26] and streptavidin [27] ligands, has shown that retention of considerable ligand flexibility in the bound state is important to achieve optimal binding. In particular, the rigidity of the  $P'_1, P'_2$  region would hinder the conformational adjustments of the inhibitor necessary to avoid the short contact of the C1 methylene and to optimise the bonding interactions with the protein.

Contrary to expectation, inhibiting properties of the diastereomeric analogue **4b** were substantially similar to that of **4a**. This result cannot be explained on the basis of the same mode of binding and could be attributed to non-specific interactions with the enzymes.

## 5. Conclusions

Conformationally constrained analogues **4a** and **4b** of endogenous pyroglutamyl tripeptide inhibitors of snake venom zinc endopeptidases proved to be inactive against adamalysin II and weak inhibitors of

MMP-2, MMP-3, MMP-8 and MMP-9. Evaluation of the hypothetical mode of binding of **4a** in the active site of these enzymes suggests that the decrease in affinity may be due to the reorientation of the acylamino chain in **3**, as shown in the crystal conformation of the ligand, and to a short contact of the C11  $\beta$ -hydrogen. In addition, the rigidity of the heterocyclic rings in the P<sub>1</sub>' and P<sub>2</sub>' region of the inhibitor, hinder the conformational adjustments necessary to avoid the short contact and to optimise the bonding interactions with the protein. These indications may be useful for the design of new non-peptidic MMPs inhibitors based on bulky groups in the P<sub>1</sub>' region.

## 6. Experimental protocols

### 6.1. Chemistry

Melting points (Büchi oil bath apparatus) are uncorrected.  $[\alpha]_D$  were determined with a Schmidt–Haensch 1604 digital polarimeter. Molecular sieves type 4A (1.7–2.4  $\mu$ m) were from Fluka Chemie AG (Buchs, Switzerland). Silica gel 60 (230–400 mesh) for column chromatography and TLC silica gel 60 F<sub>254</sub> plates were from Merck AG (Darmstadt, Germany). IR spectra were obtained with a Perkin–Elmer 16 FPC FT-IR spectrophotometer. <sup>1</sup>H NMR spectra were recorded on a Varian XL-300 spectrometer operating at 300 MHz. Chemical shifts are given in ppm relative to TMS as the internal standard. Analytical HPLC was performed on a Waters apparatus using a Vydac C<sub>18</sub> (4.6×250 mm, 30  $\mu$ m) column with CH<sub>3</sub>CN/H<sub>2</sub>O 25:75 (0.1% TFA) system as eluant (flow rate 0.5 mL min<sup>-1</sup>) with UV detection (214 nm). Reagent grade materials were from Fluka GmbH or Aldrich Chemical Co. and were used without further purification. Elemental microanalyses (C, H, N) were within  $\pm 0.4\%$  of the calculated values. Continuous fluorimetric assays were performed using a Perkin–Elmer spectrofluorimeter LS 50B.

#### 6.1.1. General procedure for preparation of the indolizino[8,7-b]indole derivatives **7a** and **7c**

A solution of trifluoroacetic acid (27 mg, 0.24 mmol) in anhydrous CH<sub>2</sub>Cl<sub>2</sub> (27 mL) was added dropwise, under stirring, to a solution of benzyl-2(*S*)-benzyloxycarbonylamino-4-oxo-butyrates [28] (4.70 g, 13.77 mmol) and L-tryptophan methylester (3.01 g, 13.77 mmol) in anhydrous CH<sub>2</sub>Cl<sub>2</sub> (160 mL) over 4 Å molecular sieves (2.8 g), cooled to 0°C, under nitrogen atmosphere. After

further stirring for 16 h at r.t., the reaction mixture was cooled to -78°C and an additional amount of trifluoroacetic acid (1.38 g, 12.1 mmol) in CH<sub>2</sub>Cl<sub>2</sub> (34 mL) was added under stirring. After 4 h at -78°C, the reaction was quenched by addition of NaHCO<sub>3</sub> saturated solution (50 mL). The organic layer was washed with brine, dried over Na<sub>2</sub>SO<sub>4</sub> and the solvent removed under reduced pressure. Purification of the crude residue (6.8 g) by silica-gel chromatography (CHCl<sub>3</sub>/*i*-PrOH 99:1 v/v) gave an unresolved mixture (4.6 g, 62%) of the two (1*S*,3*S*,2'*R*) and (1*R*,3*S*,2'*R*)-1-[2-benzyloxycarbonyl-2'-(benzyloxycarbonyl)amino]ethyl-3-methoxycarbonyl-1,2,3,4-tetrahydro- $\beta$ -carboline **6a** and **6c** (TLC: R<sub>f</sub> = 0.23 and 0.25, respectively, CHCl<sub>3</sub>/*i*-PrOH 99:1 as eluant). This material was employed for the lactamization step without further purification.

A solution of the unresolved mixture **6ac** (4 g, 7.12 mmol) in toluene (60 mL) was treated with trifluoroacetic acid (8.1 g, 71.2 mmol). The reaction mixture, after refluxing for 4 h under nitrogen, was diluted with EtOAc and washed with NaHCO<sub>3</sub> saturated solution and brine. After drying over Na<sub>2</sub>SO<sub>4</sub>, the solvents were removed under reduced pressure and the two hexahydroindolizino[8,7-*b*]indole stereoisomers **7a** and **7c** separated by silica-gel chromatography (CHCl<sub>3</sub>).

(2*R*,5*S*,11*bR*)-2-(Benzyloxycarbonyl)amino-5-methoxycarbonyl-3-oxo-2,3,5,6,11,11*b*-hexahydro-1*H*-indolizino[8,7-*b*]indole **7a** (1.977 g, 64%) was obtained (EtOAc) as white crystals: mp 220–222°C; TLC: R<sub>f</sub> = 0.13 (CHCl<sub>3</sub>/*i*-PrOH 99:1);  $[\alpha]_D^{22} = 34^\circ$  ( $c = 1$ , CHCl<sub>3</sub>); IR (KBr) main peaks at 3374, 1693, 1518, 1425, 1277, 1017, 745 cm<sup>-1</sup>; <sup>1</sup>H-NMR (DMSO-*d*<sub>6</sub>)  $\delta$  1.76 and 2.92 (2H, two m, H-1), 2.94 (1H, dd,  $J = 6.7$  and 15.5 Hz, H-6) 3.36 (1H, d,  $J = 15.5$  Hz, H-6), 3.61 (3H, s, COOCH<sub>3</sub>), 4.56 (1H, m, H-2), 4.98 (1H, m, H-11*b*), 5.04 (2H, s, Ph-CH<sub>2</sub>-O), 5.24 (1H, d,  $J = 6.7$  Hz, H-5), 6.93–7.50 (9H, m, aromatic), 7.65 (1H, d,  $J = 8.8$  Hz, NH-CO), 11.14 (1H, s, H-11). Anal. C<sub>24</sub>H<sub>23</sub>N<sub>3</sub>O<sub>5</sub> (C, H, N).

(2*R*,5*S*,11*bS*)-2-(Benzyloxycarbonyl)amino-5-methoxycarbonyl-3-oxo-2,3,5,6,11,11*b*-hexahydro-1*H*-indolizino[8,7-*b*]indole **7c** (494 mg, 16%) was obtained (MeOH) as a white solid: mp 174–176°C; TLC: R<sub>f</sub> = 0.11 (CHCl<sub>3</sub>/*i*-PrOH 99:1);  $[\alpha]_D^{22} = -92^\circ$  ( $c = 0.5$ , DMF); IR (CHCl<sub>3</sub>) main peaks at 1711, 1508, 1450, 1409, 1274, 1071, 984 cm<sup>-1</sup>; <sup>1</sup>H-NMR (DMSO-*d*<sub>6</sub>)  $\delta$  2.30 and 2.69 (2H, two m, H-1), 2.89 and 3.02 (2H, A and B of an ABX,  $J = 5.0$ , 10.9 and 15.5 Hz, H-6), 3.71 (3H, s, COOCH<sub>3</sub>), 3.94 (1H, m, H-2), 4.37 (1H, dd,  $J = 5.0$  and 10.9 Hz, H-5), 5.02 (2H, s, Ph-CH<sub>2</sub>-O), 5.09 (1H, d,

$J = 7.8$  Hz, H-11b), 6.93–7.50 (9H, m, aromatic), 7.84 (1H, d,  $J = 8.9$  Hz, NH-CO), 11.14 (1H, s, H-11). Anal.  $C_{24}H_{23}N_3O_5$  (C, H, N).

### 6.1.2. General procedure for preparation of the indolizino[8,7-b]indole derivatives **8a** and **8b**

To a suspension of the required 2-benzyloxycarbonylamino derivative **7a** or **7b** [19] (1 mmol) and 10% Pd/C (100 mg) in MeOH (10 mL), ammonium formate (4 mmol) was added at r.t., under rapid stirring. After 10 min, the reaction mixture was filtered through a short celite pad and the solvent removed under reduced pressure. Washing with water of the resulting solid residue gave the deprotected 2-amino derivative that was dried in high vacuum and dissolved in anhydrous DMF (4.6 mL) together with furan-2-carboxylic acid (1 mmol) and 1-hydroxybenzotriazole (1 mmol). The mixture was treated with a solution of dicyclohexylcarbodiimide (1.1 mmol) in DMF (2.3 mL) for 1 h at 0°C and 1 h at 25°C and the solvent removed under reduced pressure. The crude residue was stirred in EtOAc (10 mL), the dicyclohexylurea filtered off and the solution washed with 1 M citric acid, 1 M  $NaHCO_3$  and brine. The organic layer was dried over  $Na_2SO_4$  and the solvent removed under reduced pressure. Silica gel chromatography ( $CHCl_3/i$ -PrOH 99:1) of the crude residue and crystallization from MeOH gave the pure products.

(2*R*,5*S*,11*bR*)-2-(Furan-2-carbonyl)amino-5-methoxycarbonyl-3-oxo-2,3,5,6,11,11*b*-hexahydro-1*H*-indolizino [8,7-*b*]indole **8a** (275 mg, 70%), mp 150–153°C; TLC:  $R_f = 0.18$  ( $CHCl_3/i$ -PrOH 99:1);  $[\alpha]_D^{25} = 54^\circ$  ( $c = 1$ ,  $CHCl_3$ ); IR ( $CHCl_3$ ) main peaks at 3464, 1704, 1595, 1508 1420, 1300, 1010,  $cm^{-1}$ ;  $^1H$ -NMR (DMSO- $d_6$ )  $\delta$ 1.95 and 2.96 (2H, two m, H-1), 2.98 (1H, dd,  $J = 6.7$  and 15.5 Hz, H-6) 3.35 (1H, d,  $J = 15.5$  Hz, H-6), 3.64 (3H, s,  $COOCH_3$ ), 5.01 (1H, m, H-11*b*), 5.03 (1H, m, H-2), 5.27 (1H, d,  $J = 6.7$  Hz, H-5), 6.58–7.94 (7H, m, aromatic and furan), 8.71 (1H, d,  $J = 8.7$  Hz, NH-CO), 11.14 (1H, s, H-11). Anal.  $C_{21}H_{19}N_3O_5$  (C, H, N).

(2*R*,5*S*,11*bS*)-2-(Furan-2-carbonyl)amino-5-methoxycarbonyl-3-oxo-2,3,5,6,11,11*b*-hexahydro-1*H*-indolizino [8,7-*b*]indole **8b** (197 mg, 50%); mp 290–294°C; TLC:  $R_f = 0.16$  ( $CHCl_3/i$ -PrOH 99:1);  $[\alpha]_D^{25} = 20^\circ$  ( $c = 0.5$ , DMF); IR ( $CHCl_3$ ) main peaks at 1702, 1594, 1516, 1421, 1304, 1173, 1012  $cm^{-1}$ ;  $^1H$ -NMR (DMSO- $d_6$ )  $\delta$ 2.48 (2H, two m, H-1), 3.04 (1H, dd,  $J = 7.2$  and 15.8 Hz, H-6), 3.22 (1H, d,  $J = 15.8$  Hz, H-6), 3.66 (3H, s,  $COOCH_3$ ), 4.52 (1H, m, H-2), 5.27 (2H, m, H-5 and H-11*b*) 6.60–7.96 (7H, m, aromatic and furan), 9.04

(1H, d,  $J = 8.3$  Hz, NH-CO), 11.15 (1H, s, H-11). Anal.  $C_{21}H_{19}N_3O_5$  (C, H, N).

### 6.1.3. Hydrolysis of the 5-methoxycarbonylhexahydroindolizino[8,7-*b*]indole derivatives **8a** and **8b**

A suspension of the required ester (1 mmol) in 3:1 dioxane/methanol (9 mL) was treated with aqueous 2 N NaOH (1 mL) and stirred overnight at r.t. The reaction mixture was diluted with water (35 mL) and washed with EtOAc. The aqueous layer was cooled in ice, acidified with 2 N HCl to pH 3 and extracted with  $CHCl_3$  ( $2 \times 20$  mL). After washing with brine and drying over  $Na_2SO_4$ , the organic phase was evaporated under reduced pressure to give the pure product **4a** or **4b**.

(2*R*,5*S*,11*bR*)-2-(Furan-2-carbonyl)amino-5-carboxy-3-oxo-2,3,5,6,11,11*b*-hexahydro-1*H*-indolizino [8,7-*b*]indole **4a** (239 mg, 70%), mp 195–198°C; HPLC:  $t_R = 19.60$  min;  $[\alpha]_D^{25} = 126^\circ$  ( $c = 0.5$ , DMF); IR (KBr) main peaks at 3394, 1692, 1530, 1428, 1296, 1205, 758,  $cm^{-1}$ ;  $^1H$ -NMR (DMSO- $d_6$ )  $\delta$ 1.95 and 2.96 (2H, two m, H-1), 2.98 (1H, dd,  $J = 6.7$  and 15.5 Hz, H-6) 3.35 (1H, d,  $J = 15.5$  Hz, H-6), 3.64 (3H, s,  $COOCH_3$ ), 5.01 (1H, m, H-11*b*), 5.03 (1H, m, H-2), 5.27 (1H, d,  $J = 6.7$  Hz, H-5), 6.58–7.94 (7H, m, aromatic and furan), 8.71 (1H, d,  $J = 8.7$  Hz, NH-CO), 11.14 (1H, s, H-11). Anal.  $C_{20}H_{17}N_3O_5$  (C, H, N).

(2*R*,5*S*,11*bS*)-2-(Furan-2-carbonyl)amino-5-carboxy-3-oxo-2,3,5,6,11,11*b*-hexahydro-1*H*-indolizino [8,7-*b*]indole **4b** (360 mg, 95%); mp 270–275°C; HPLC:  $t_R = 19.60$  min;  $[\alpha]_D^{25} = 48^\circ$  ( $c = 0.5$ , DMF); IR (KBr) main peaks at 3271, 1647, 1593, 1527, 1429, 1318, 1203,  $cm^{-1}$ ;  $^1H$ -NMR (DMSO- $d_6$ )  $\delta$ 2.48 (2H, two m, H-1), 3.04 (1H, dd,  $J = 7.2$  and 15.8 Hz, H-6), 3.22 (1H, d,  $J = 15.8$  Hz, H-6), 3.66 (3H, s,  $COOCH_3$ ), 4.52 (1H, m, H-2), 5.27 (2H, m, 5-H and H-11*b*) 6.60–7.96 (7H, m, aromatic and furan), 9.04 (1H, d,  $J = 8.3$  Hz, NH-CO), 11.15 (1H, s, H-11). Anal.  $C_{20}H_{17}N_3O_5$  (C, H, N).

## 6.2. Structural studies

### 6.2.1. X-ray data collection and reduction

Crystals of **4a** were obtained from a methanol solution by slow evaporation. X-ray data were collected at room temperature on a Rigaku AFC5R diffractometer with graphite monochromated Cu  $K\alpha$  radiation and a 12 kW rotating anode generator. Cell constants and the orientation matrix for data collection were obtained from a least square fit of the angular settings of 20 carefully centred reflections in the range  $26.5^\circ < 2\theta < 42.8^\circ$ . The cell parameters, refined on higher angle

reflections, are reported in *table II*. Intensity data were collected by the  $\omega/2\theta$  scan technique with scans of  $(1+0.3 \text{ tg}\theta)^\circ$  at variable and appropriate speed to a maximum  $2\theta$  of  $124^\circ$ . Stationary background counts were recorded on each side of the reflection. The peak counting was twice that of the background. Reflections with  $I < 25\sigma(I)$  were rescanned with accumulation of counts to improve counting statistics. Out of 1681 reflections, 1099 had  $I > 3\sigma(I)$  and were used in the refinement. The intensities of three standard reflections, measured after every 147 reflections declined by 7.7%; a linear correlation factor was applied to the data to account for this. An empirical absorption correction, based on azimuthal scans of several reflections, was applied resulting in transmission factors ranging from 0.92 to 1.00. The data were corrected for Lorentz and polarization effects. A correction for secondary extinction was finally applied (coefficient =  $2.7 \times 10^{-6}$ ).

### 6.2.2. Structure solution and refinement

The structure was solved by direct methods using the program SIR92 [29] and successive Fourier maps. The non-H atoms were refined anisotropically by full-matrix least-squares method. The function minimized was

$\sum w(|F_o| - |F_c|)^2$  where  $w = 4 F_o^2 / \sigma^2(F_o^2)$ . All the H atoms were located at the expected positions except the carboxyl group, which was detected from the final difference Fourier map. The H-atoms were included in the last structure factor calculation with isotropic thermal parameters deduced from the carrier atoms. The final  $R$  and  $R_w$  are 0.043 and 0.046, respectively. The atomic scattering factors were those of Cromer and Mann [30]. Anomalous dispersion effects were taken into account adopting  $\Delta f'$  and  $\Delta f''$  values of Cromer [31]. The final fractional coordinates of the non-H atoms together with their  $B_{\text{eq}}$  and individual e.s.d.s are given in *table III*.

All calculations were performed using TEXSAN [32] crystallographic software package.

A list of H atom coordinates, non-H atom anisotropic parameters, valence bond lengths and angles, torsion angles and observed and calculated structure factors are available on request to the authors.

### 6.2.3. Matrix metalloproteinases activation and inhibition assays

The proenzymes [33] were activated immediately prior to use with *p*-aminophenylmercuric acetate (APMA 1 mM for 1 h at  $25^\circ$  for pro-MMP-2 and pro-MMP-9 [34]; with APMA 2 mM for 2 h at  $37^\circ\text{C}$  for pro-MMP-8 [35] and with  $\alpha$ -chymotrypsin  $6 \mu\text{g mL}^{-1}$  for 2 h at  $37^\circ\text{C}$  followed by phenylmethylsulfonyl fluoride 0.2 mM for pro-MMP-3 [36].

For assays measurements, 0.05 mM solutions of the inhibitors in MeOH were further diluted as required in the assay buffer, Tris 100 mM, NaCl 100 mM,  $\text{CaCl}_2$  10 mM, pH 7.5, Brij 35 0.05%. The activated enzyme plus inhibitor (13  $\mu\text{M}$  final concentration) solution was incubated in the assay buffer for 3 h. The assay temperature was  $25^\circ\text{C}$  for MMP-2 and MMP-9 and  $37^\circ\text{C}$  for MMP-3 and MMP-8. After the addition of 0.1 or 0.05 mM solution of the appropriate fluorogenic substrate [37] in DMSO, the hydrolysis was monitored [38] by continuously recording the increase in fluorescence ( $\lambda_{\text{ex}}$  328 nm,  $\lambda_{\text{em}}$  393 nm) using a Perkin–Elmer spectrofluorimeter LS 50B. Percent inhibitions were calculated from control reactions without the inhibitor as means of at least three independent measurements.

### 6.2.4. Adamalysin II inhibition assay

Similarly to the previous procedure, adamalysin II [33] (6  $\mu\text{g}$ ) in the assay buffer (Tris–HCl 50 mM,  $\text{CaCl}_2$  10 mM, pH 7.5) plus 0.05 mM inhibitor solution in MeOH, was immediately added with a solution of 2-aminobenzoyl–Ala–Gly–Leu–Ala–*p*-nitrobenzylamide

**Table II.** Crystal data of **4a**<sup>a</sup>

Empirical formula	$\text{C}_{20}\text{H}_{17}\text{N}_3\text{O}_5$
Formula weight	379.4
Crystal system	Orthorhombic
$a$ (Å)	9.745(2)
$b$ (Å)	27.131(5)
$c$ (Å)	6.735(2)
$V$ (Å <sup>3</sup> )	1780.7(8)
Space group	$P2_1 2_1 2_1$
$d_c$ (g cm <sup>-3</sup> )	1.415
$Z$	4
$F(000)$	792
$\lambda$ (Cu K $\alpha$ ) (Å)	1.5418
$\mu$ (Cu K $\alpha$ ) (mm <sup>-1</sup> )	0.8
Crystal size (mm)	$0.2 \times 0.3 \times 0.01$
$2\theta_{\text{max}}$ (°)	124
No. reflections [ $I > 3\sigma(I)$ ]	1099
$R, R_w$	0.043, 0.046
Weighting scheme	$4 F_o^2 / \sigma^2(F_o^2)$
$S$	1.4
Observation/parameter	4.3
Max. min peak in the final difference map (e Å <sup>-3</sup> )	0.17, -0.19

<sup>a</sup> Maximum resolution of collected data is given by the  $2\theta_{\text{max}}$  (°) value.

**Table III.** Fractional coordinates and  $B_{\text{(eq)}}$  with their e.s.d.s, in parentheses, for **4a**

Atom	<i>x</i>	<i>y</i>	<i>z</i>	$B_{\text{(eq)}}$
C(1)	0.7036 (6)	0.9222 (2)	0.9464 (8)	3.4 (3)
C(2)	0.7201 (5)	0.9593 (2)	0.7791 (8)	2.8 (3)
C(3)	0.5759 (6)	0.9630 (2)	0.686 (1)	2.8 (3)
C(5)	0.3465 (5)	0.9301 (2)	0.7507 (8)	2.9 (3)
C(6)	0.3252 (6)	0.8740 (2)	0.7462 (8)	3.4 (3)
C(7)	0.2684 (6)	0.7657 (2)	0.983 (1)	4.5 (3)
C(8)	0.2596 (8)	0.7280 (2)	1.118 (1)	6.2 (4)
C(9)	0.3393 (8)	0.7275 (2)	1.287 (1)	6.7 (5)
C(10)	0.4329 (7)	0.7644 (2)	1.326 (1)	5.3 (4)
C(11)	0.5472 (5)	0.9222 (2)	0.9922 (9)	2.8 (2)
C(12)	0.3894 (5)	0.8506 (2)	0.9247 (8)	2.9 (3)
C(13)	0.3602 (6)	0.8047 (2)	1.021 (1)	3.1 (3)
C(14)	0.4407 (6)	0.8025 (2)	1.192 (1)	3.4 (3)
C(16)	0.4860 (5)	0.8729 (2)	1.0345 (8)	2.7 (2)
C(17)	0.2528 (6)	0.9571 (2)	0.895 (1)	3.4 (3)
C(20)	0.8019 (6)	0.9065 (2)	0.5159 (9)	3.1 (3)
C(21)	0.9211 (7)	0.8910 (2)	0.399 (1)	3.9 (3)
C(22)	1.0479 (6)	0.9080 (2)	0.384 (1)	4.4 (3)
C(23)	1.1188 (8)	0.8746 (4)	0.260 (1)	7.2 (5)
C(24)	1.030 (1)	0.8402 (3)	0.204 (1)	8.1 (6)
N(4)	0.4886 (4)	0.9408 (1)	0.8057 (7)	2.8 (2)
N(15)	0.5189 (5)	0.8456 (2)	1.1983 (7)	3.4 (2)
N(19)	0.8224 (4)	0.9458 (1)	0.6352 (7)	2.9 (2)
O(3)	0.5507 (4)	0.9846 (1)	0.5305 (6)	3.5 (2)
O(17)	0.2927 (4)	0.9836 (1)	1.0232 (8)	5.8 (2)
O(18)	0.1204 (4)	0.9496 (1)	0.8575 (6)	3.8 (2)
O(20)	0.6909 (4)	0.8851 (1)	0.5081 (7)	3.9 (2)
O(25)	0.9029 (5)	0.8489 (2)	0.2895 (8)	6.5 (3)

[39] in MeOH (1.5  $\mu\text{M}$ , final concentration. Hydrolysis of the fluorogenic substrate was monitored by continuously recording the increase in fluorescence ( $\lambda_{\text{ex}}$  320 nm,  $\lambda_{\text{em}}$  420 nm) for 30 min at 30°C.

### Acknowledgements

The authors wish to thank M. Petrilli and F. Dianetti, Servizio Microanalisi del CNR, Area della Ricerca di Roma, Montelibretti, who performed elemental microanalyses. This work was supported by Italian CNR Targeted Program Biotecnologie, MURST and Cofin. MURST 97 CFSIB.

### References

- [1] Woessner J.F., *FASEB J.* 5 (1991) 2145–2154.  
 [2] Morphy J.R., Millican T.A., Porter J.R., *Curr. Med. Chem.* 2 (1995) 743–762.

- [3] Hagman W.K., Lark M.V., Becker J.W., *Ann. Rep. Med. Chem.* 31 (1996) 231–240.  
 [4] Ye Q.Z., Hupe D., Johnson L., *Curr. Med. Chem.* 3 (1996) 407–418.  
 [5] Levy D.E., Ezrin A., *Emerging Drugs* 2 (1997) 205–230.  
 [6] Schwartz M.A., Van Wart H.E., in: Ellis G.P., Luscombe D.K. (Eds.), *Progress in Medicinal Chemistry*, vol. 29, Elsevier, Amsterdam, 1991, pp. 239–270.  
 [7] Porter J.R., Millican T.A., Morphy J.R., *Exp. Op. Ther. Pat.* 5 (1995) 1287–1296.  
 [8] Becket R.P., Davidson A.H., Drummond D.H., Huxley P., Whittaker M., *Drug Discov. Today* 1 (1996) 16–26.  
 [9] Becket R.P., *Exp. Op. Ther. Pat.* 6 (1996) 1305–1315.  
 [10] Becket R.P., Whittaker M., *Exp. Op. Ther. Pat.* 8 (1998) 259–282.  
 [11] Stöcker W., Grams S., Baumann U., Reinemez P., Gomis-Rüth F.X., McKay D.B., Bode W., *Prot. Sci.* 4 (1995) 823–840.  
 [12] Gomis-Rüth F.X., Kress L.F., Bode W., *EMBO J.* 12 (1993) 4151–4157.  
 [13] Gomis-Rüth F.X., Kress L.F., Kellerman J., Moyr I., Lee X., Huber R., Bode W., *J. Mol. Biol.* 239 (1994) 513–544.  
 [14] Fox J.W., Bjarnason J.B., in: Bailey G.S. (Ed.), *Enzymes from Snake Venom*, Alaken, Fort Collins, CO, 1998, pp. 599–632.  
 [15] Robeva A., Politi V., Shannon J.D., Bjarnason J.B., Fox J.W., *Biomed. Biochim. Acta* 50 (1991) 769–773.  
 [16] Zhang D., Botos I., Gomis-Rüth F.X., Doll R., Blood C., Njoroge F.G., Fox J.W., Bode W., Meyer F., *Proc. Natl. Acad. Sci. USA* 91 (1994) 8447–8451.  
 [17] Cirilli M., Gallina C., Gavuzzo E., Giordano C., Gomis-Rüth F.X., Gorini B., Kress L.F., Mazza F., Paglialunga-Paradisi M., Pochetti G., Politi V., *FEBS Letts.* 418 (1997) 319–322.  
 [18] Gomis-Rüth F.X., Meyer E.F., Kress L.F., Bode W., Politi V., *Prot. Sci.* 7 (1998) 283–292.  
 [19] De la Figuera N., Alkorta I., Garcia Lopez M.T., Herranz R., Gonzáles Muñiz R., *Tetrahedron* 51 (1995) 7841–7856.  
 [20] Bailey P.D., Hollinshead S.P., McLay N.R., Morgan K., Palmer S.J., Prince S.N., Reynolds C.D., Wood S.D., *J. Chem. Soc. Perkin Trans. 1* (1993) 431–439.  
 [21] Melnyk P., Ducrot P., Thal C., *Tetrahedron* 49 (1993) 8589–8596.  
 [22] König W., Geiger R., *Chem. Ber.* 103 (1970) 788–798.  
 [23] Fairlie D.P., Tyndall J.D.A., Reid R.C., Wong A.K., Abbenante G., Scanlon M.J., March D.R., Bergman D.A., Chai C.L.L., Burkett B.A., *J. Med. Chem.* 43 (2000) 1271–1281.  
 [24] As observed by one of the referees, the analogue of **4a** with C11*b* in the *R* configuration, would render the C1 atom 'above' the plane approximately formed by C11*b*, N4, C3 and C2 in ring D (figure 3), allowing more rotational flexibility to bond C2–N19 and therefore more freedom for the furan-2-carboxamide group. Synthesis of this compound was included in the original plan of the work and the corresponding methylester was also prepared. Unfortunately, hydrolysis under the usual, mild, alkaline conditions caused extensive isomerization (possibly epimerization at C5). From the resulting mixture of carboxylic acids, we failed to isolate the pure substances in adequate amount for characterization.  
 [25] Babine E., Bender S.L., *Chem. Rev.* 97 (1997) 1359–1472.

- [26] Yiotakis A., Lecoq A., Vassiliou S., Raynal I., Cuniassé P., *J. Med. Chem.* 37 (1994) 2713–2720.
- [27] Weber P.C., Pantoliano M.W., Simons D.M., Salemme F.R., *J. Am. Chem. Soc.* 116 (1994) 2717–2724.
- [28] Prepared by oxydation of *N*-benzyloxycarbonyl-D-homoserine according to Keith D.D., Tortora J.A., Ineichen K., Leimgruber W., *Tetrahedron* 31 (1975) 2633–2636.
- [29] Altomare A., Cascarano G., Giacobozzo C., Guagliardi A., Burla M.C., Polidori G., Camalli M., *J. Appl. Cryst.* 27 (1994) 435.
- [30] Cromer D.T., Waber J.T., *International Tables for X-ray Crystallography*, vol. IV, Kynock Press, Birmingham, UK, 1974 Table 2.2A.
- [31] Cromer D.T., Waber J.T., *International Tables for X-ray Crystallography*, vol. IV, Kynock Press, Birmingham, UK, 1974 Table 2.3.1.
- [32] TEXSAN: TEXRAY Structure Analysis Package, Molecular Structure Corporation, 1985.
- [33] Pro-MMP-2, pro-MMP-3, pro-MMP-8 and pro-MMP-9 were supplied by G. Murphy (Strangeways Research Laboratories, Cambridge, UK). Adamalysin II was a kind gift from L.F. Kress (Roswell Park Cancer Institute, Buffalo, New York).
- [34] Murphy G., Crabbe T., *Methods Enzymol.* 248 (1995) 470–484.
- [35] Tschesche H., *Methods Enzymol.* 248 (1995) 431–439.
- [36] Nagase H., *Methods Enzymol.* 248 (1995) 449–470.
- [37] Fluorogenic substrates (7-methoxycoumarin-4-yl)acetyl-Pro-Leu-Gly-Leu-(3-[2,4-dinitro-phenyl]-L-2,3-diaminopropionyl) × -Ala-Arg-NH<sub>2</sub> (MCA-Pro-Leu-Gly-Leu-Dpa-Ala-Arg-NH<sub>2</sub>) Ref. 33 for MMP-2 and MMP-9, MCA-Pro-Cha-Gly-Nva-His-Ala-Dpa-NH<sub>2</sub> for MMP-3 (Knight, C.G., private communication) and MCA-Pro-Leu-Ala-Nva-Dpa-Ala-Arg-NH<sub>2</sub> for MMP-3 (Knight C.G., private communication) were supplied by Knight C.G. (Strangeways Research Laboratories, Cambridge, UK). 2-Aminibenzoyl-Ala-Gly-Leu-Ala-*p*-nitrobenzylamide was purchased from Bachem (Budendorf, Switzerland).
- [38] Knight C.G., Willenbrock F., Murphy G., *FEBS Letts.* 296 (1992) 263–266.
- [39] Fox J.W., Campbell R., Beggerly L., Bjarnason J.B., *Eur. J. Biochem.* 156 (1986) 65–72.